





## Carbon accumulation rates are highest at young and expanding salt marsh edges

Carson B. Miller <sup>1,2</sup>, Antonio B. Rodriguez <sup>1,2</sup>✉, Molly C. Bost <sup>1,2</sup>, Brent A. McKee<sup>2</sup> & Nathan D. McTigue <sup>3</sup>

An objective of salt marsh conservation, restoration, and creation is to reduce global carbon dioxide levels and offset emissions. This strategy hinges on measurements of salt marsh carbon accumulation rates, which vary widely creating uncertainty in monetizing carbon credits. Here, we show the 14–323 g C m<sup>-2</sup> yr<sup>-1</sup> range of carbon accumulation rates, derived from cores collected at seven sites in North Carolina U.S.A., results from the landward or basinward trajectory of salt marsh colonization and the intertidal space available for accretion. Rates increase with accelerating sea-level rise and are highest at young and expanding marsh edges. The highest carbon densities are near the upland, highlighting the importance of this area for building a rich stock of carbon that would be prevented by upland development. Explaining variability in carbon accumulation rates clarifies appraisal of salt marsh restoration projects and landscape conversion, in terms of mitigating green-house gas emissions.

<sup>1</sup>Institute of Marine Sciences, University of North Carolina at Chapel Hill, 3431 Arendell St., Morehead City, NC 28557, USA. <sup>2</sup>Earth, Marine, and Environmental Sciences, University of North Carolina at Chapel Hill, Chapel Hill, NC 27599-3300, USA. <sup>3</sup>The University of Texas at Austin, Marine Science Institute, Port Aransas, TX 78373, USA. ✉email: [abrodrig@email.unc.edu](mailto:abrodrig@email.unc.edu)

Carbon markets allow individuals and corporations to offset their greenhouse gas emissions by purchasing carbon credits generated by projects that reduce greenhouse gases elsewhere. Many projects create carbon credits through biological sequestration, such as afforestation and reforestation<sup>1</sup>. Restoring coastal ecosystems such as salt marshes to sequester carbon has potential for generating carbon credits<sup>2</sup>; however, estimates of salt marsh carbon accumulation rates (CAR) vary globally from 1.2 to 1167.5 g C m<sup>-2</sup> yr<sup>-1</sup> (average of 167.7 ± 136.5 g C m<sup>-2</sup> yr<sup>-1</sup>; ± 1 SD)<sup>3</sup>. The large range of salt marsh CARs creates uncertainty in upscaling measurements, monetizing carbon credits, appraising the value of restoration and conservation projects, and would add speculation to the carbon market<sup>4</sup>.

Salt marsh has a great capacity for accumulating and storing atmospheric carbon in its soil as compared to other coastal and terrestrial vegetated habitats<sup>5</sup>. A large stock of carbon is stored below ground as salt marsh organic carbon and continuously accumulates over centuries to millennia<sup>6,7</sup>. Assuming CAR will remain constant, and the previously stored blue carbon will remain out of the atmosphere for climate-relevant periods is problematic<sup>8,9</sup> because globally salt marsh is decreasing via conversion to other landscapes, such as open water or agricultural fields, at 1.0–2.0% yr<sup>-1</sup><sup>10</sup>. Salt marsh conversion is commonly associated with erosion of the carbon stock (the carbon stored in the salt marsh sedimentary unit) and re-release of carbon into the atmosphere<sup>10–12</sup>. The carbon stock that many salt marshes have stored is mainly a result of the rapid accumulation of organic-carbon rich sediments and conditions that promote preservation of organic carbon. Rapid vertical accretion of salt marsh sediments is driven by ecogeomorphic feedbacks that maintain surface elevation in the tidal frame by promoting sediment accumulation of both inorganic and organic fractions at rates equivalent to relative sea-level rise (RSLR)<sup>13,14</sup>. Preservation of organic carbon is optimized by the biogeochemistry of salt marsh soil that restricts oxic and suboxic degradation to shallow depths (<20 cm)<sup>15,16</sup>.

Salt marsh CAR variability has been shown to be broadly driven by regional differences in latitude (highest mean value at lower latitudes), tidal range (higher values in micro-tidal settings), elevation (higher values at lower elevations), and dominant halophyte genera (highest for *Spartina alterniflora*); however, saltmarsh CAR is still highly variable within regions<sup>3,6,17</sup>. The

time scale over which salt marsh CAR is measured is the most important factor contributing to the large reported global range. Measurements that integrate over yearly to decadal short time scales using sediment-trap and marker-bed methods produce the highest values and span the entire two-orders of magnitude range<sup>18</sup>. Quantifying salt marsh CAR by integrating over short time scales skews values higher for three main reasons, including: (1) diagenesis of organic matter occurs during burial not short-term deposition<sup>16,19</sup>, (2) maximum belowground production of organic carbon (roots and rhizomes) is at shallow depths, typically <15 cm, which comprises most of the sediment from which short-term rates are based<sup>20,21</sup>, and (3) accelerating relative sea-level rise (RSLR) enhances salt marsh CAR<sup>3,8,22,23</sup>, and the average rate of sea-level rise over the past century was greater than the previous millennium<sup>24</sup>.

Salt marsh forms in a variety of low-energy estuarine settings such as fringing upland supratidal environments (forests) and colonizing intertidal substrates away from shorelines (tidal flats and oyster reefs) forming patches<sup>25</sup>. Fringing salt marsh, the most extensive estuarine salt marsh setting, is the focus of our study because it continues to form as RSLR inundates upland areas (if unimpeded by development) and it is typically targeted for restoration and conservation<sup>26–29</sup>. The two edges of fringing marsh include its contact with the upland and the estuarine shoreline, and both move laterally through time as the salt marsh responds to changes in water level, hydrodynamic energy, and sedimentation. The upland boundary of fringing salt marsh moves landward with RSLR (transgression) and if sediment supply is high enough, saltmarsh can also expand into the estuary (regression; Fig. 1). Salt marsh area increases with salt marsh transgression and regression and decreases with upland regression, shoreline erosion, and salt marsh submergence.

Salt marsh transgression rates are principally modulated by the upland surface gradient and the rate of RSLR because those factors determine the landward extent of soil salinization, which leads to forest degradation and salt marsh encroachment<sup>30–33</sup>. Storms have also been recognized as important drivers of salt marsh transgression by facilitating tree mortality, inundating forest soil with saline storm-surge water, and producing shallow subsidence through organic matter degradation<sup>32,34,35</sup>. At the upland boundary, RSLR provides the space (accommodation) for salt marsh sediment to accumulate in. The salt marsh estuarine shoreline moves landward as it is eroded by waves and currents,

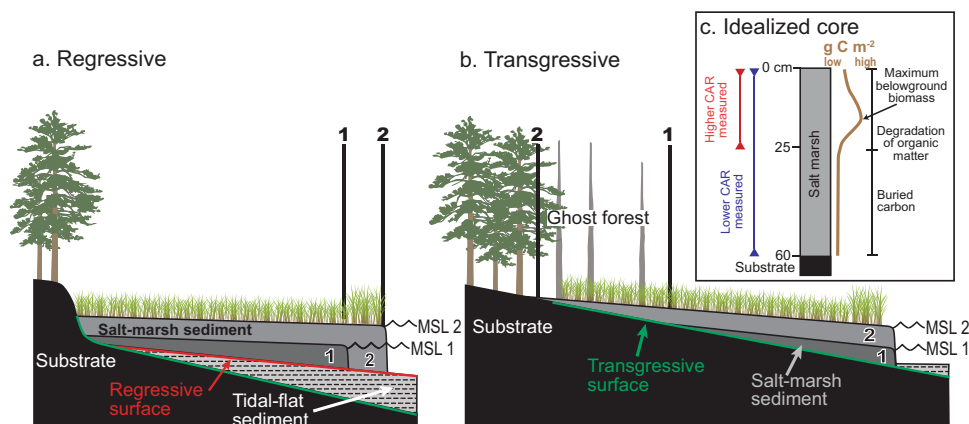


**Fig. 1** Conceptual models illustrating fringing salt marsh ontogeny and carbon burial with sea-level rise. The shoreline of a regressive salt marsh moves into the estuary (basinward; **a**) and the landward edge of a transgressive salt marsh moves into the upland (landward; **b**) with sea-level rise from time 1–2. These models represent the types of salt marshes examined in this study; however, other salt marshes are accreting at rates <sea-level rise, have eroding shorelines, or are expanding in both landward and basinward directions. A typical down-core profile of carbon storage in a salt marsh (**c**) illustrating the higher and lower carbon accumulation rates that result from integrating over short (0–25 cm) and long (0–60 cm) intervals and associated time scales, respectively. Depths shown are hypothetical and vary among and within salt marshes.

but it can also regress into the estuary. Salt marsh regression is primarily controlled by base level, sediment supply, and near-shore bathymetry. Sediments accumulate below base level, and in estuaries the depth of base level is primarily controlled by wave base, tidal currents, and relative sea level. Elevating base level through RSLR and decreasing hydrodynamic energy adjacent to the salt marsh shoreline produces accommodation for sediments to accumulate in. This accommodation is initially filled with tidal-flat sediments that can raise the elevation of the sediment surface to a level conducive for salt marsh colonization and regression<sup>36,37</sup>. At the regressive shoreline, salt marsh initially forms at its lowest possible growth elevation and sediment accommodation is at a maximum, in contrast to the upland boundary where salt marsh initially forms at its highest possible growth elevation and sediment accommodation is at a minimum and limited to RSLR.

Spatial and temporal variations in salt marsh sediment accommodation, which is strongly linked to the ontogeny of a salt marsh, should be reflected in salt marsh CAR. We hypothesize that the large range of salt marsh CAR integrated across various time scales of measurement within regions is masking well-defined globally relevant patterns related to ontogeny, landscape setting, and RSLR. To test this, we collected a transect of cores from the upland boundary to the estuarine shoreline at seven

microtidal fringing salt marshes in North Carolina, U.S.A. By applying a consistent method for measuring CAR that includes the entire salt marsh sedimentary unit, here, we show clear spatial and temporal patterns exist that are directly related to salt marsh ontogeny. Explaining the drivers of salt marsh CAR variability, beyond broad regional groupings and time scales of interest, is important for accurate carbon pricing and qualifying expectations for the effectiveness of restoration projects at mitigating greenhouse-gas emissions through time.

## Results and discussion

The transgressive ( $n = 3$ ) and regressive ( $n = 4$ ) salt marshes (Fig. 2) were initially defined by stratigraphic patterns, with a salt marsh unit overlying an upland soil being transgressive and a salt marsh unit overlying an adjacent estuarine mudflat or sandflat being regressive. Every core ( $n = 51$ ) sampled the entire salt marsh, underlying Holocene strata, and the top of basal undifferentiated Pleistocene strata (Supplementary Fig. 1). Regressive salt marshes were separated from the upland by a 1–2 m step, had a mean width of  $53 \pm 24$  m (1 SD), and most were dominated by *Spartina alterniflora* (not NPR-U; Fig. 2; Table 1). Transgressive salt marshes were dominated by *Juncus roemerianus*, had a low gradient upland boundary transition zone, and a mean width of

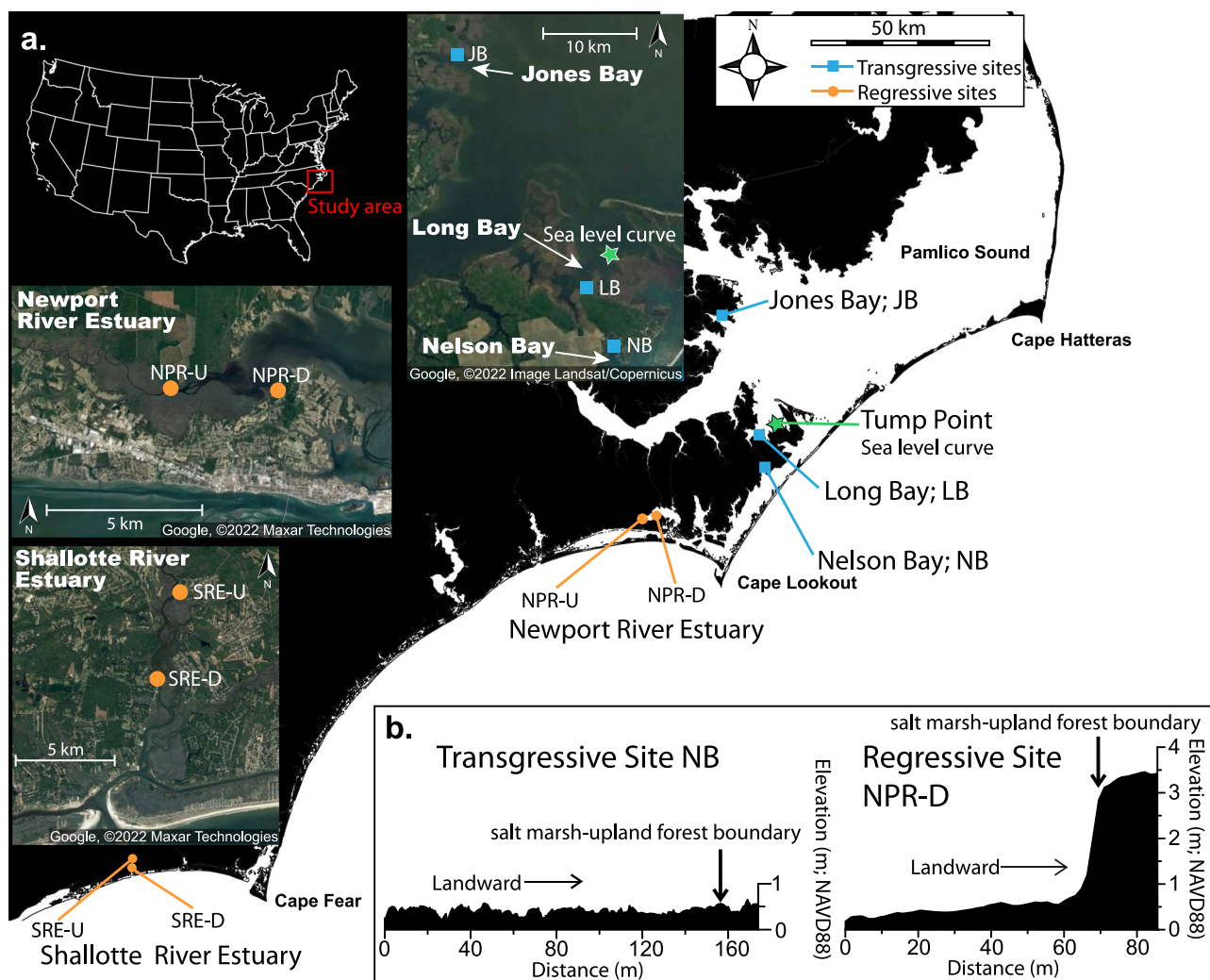


**Fig. 2** Location of study sites in North Carolina, USA. Transgressive and regressive fringing salt marsh sites are located north and west of Cape Lookout, respectively (a). Representative topographic profiles (b) showing low gradient upland and wide salt marsh at transgressive sites (Nelson Bay NB) and high gradient upland and narrow salt marsh at regressive sites (Newport River Estuary NPR-D). The Tump Point sea-level curve is indicated by the green star<sup>38</sup>.

**Table 1** Sampling site information and marsh sedimentary unit measurements.

Site Name; Core #	Species	Development Mode	Sampling Year (CE)	Easting	Northing	Elev. (m; NAVD88)	Thickness (m)	Date (CE) <sup>a</sup>	C Stock (g m <sup>-2</sup> ) <sup>b</sup>
NPR-D; 8	<i>Spartina</i>	Regressive	2018	341061	3847425	0.17	0.53	2003	5013 ± 150
NPR-D; 14	<i>Spartina</i>	Regressive	2018	341098	3847406	0.32	0.36	1971	3482 ± 104
NPR-D; 16	<i>Spartina</i>	Regressive	2018	341106	3847402	0.39	0.42	1967	4346 ± 130
NPR-U; 5	<i>Juncus</i>	Regressive	2019	337270	3847270	0.45	0.75	1415	14520 ± 436
NPR-U; 1	<i>Juncus</i>	Regressive	2019	337263	3847247	0.53	1.02	1588	1212 ± 364
SRE-U; 6	<i>Spartina</i>	Regressive	2019	743692	3760253	0.18	0.6	1443	8024 ± 241
SRE-U; 1	<i>Spartina</i>	Regressive	2019	743648	3760206	0.50	0.8	1783	10762 ± 323
SRE-D; 1	<i>Spartina</i>	Regressive	2018	743213	3758113	−0.23	0.31	1966	2849 ± 85
NB; 1	<i>Juncus</i>	Transgressive	2018	371264	3859486	0.21	0.51	1957	11275 ± 338
NB; 3	<i>Juncus</i>	Transgressive	2018	371199	3859505	0.19	0.21	1962	6327 ± 190
NB; 9	<i>Juncus</i>	Transgressive	2018	371232	3859496	0.11	0.31	1962	6691 ± 201
JB; 1	<i>Juncus</i>	Transgressive	2018	360457	3899959	0.21	0.9	1557	19765 ± 593
JB; 5	<i>Juncus</i>	Transgressive	2018	360460	3900004	0.09	1.01	1662	22916 ± 687
JB; 7	<i>Juncus</i>	Transgressive	2018	360449	3900099	0.07	0.58	1783	13027 ± 391
JB; 6	<i>Juncus</i>	Transgressive	2018	360459	3900063	0.09	0.82	1551	17633 ± 529
JB; 8	<i>Juncus</i>	Transgressive	2018	360442	3900130	0.03	0.27	1973	7350 ± 221
LB; 3	<i>Juncus</i>	Transgressive	2019	369226	3867912	0.22	1.24	1247	21647 ± 649
LB; 5	<i>Juncus</i>	Transgressive	2019	369285	3867775	0.17	0.83	1335	19197 ± 576
LB; 6	<i>Juncus</i>	Transgressive	2019	369316	3867697	0.19	0.8	1589	15833 ± 475
LB; 7	<i>Juncus</i>	Transgressive	2019	369327	3867653	0.23	0.51	1850	12040 ± 361
LB; 8	<i>Juncus</i>	Transgressive	2019	369336	3867617	0.24	0.25	1893	7418 ± 223
LB; 9	<i>Juncus</i>	Transgressive	2019	369347	3867579	0.24	0.31	1957	8424 ± 253

<sup>a</sup> Median date. See Supplementary Data 1 for details.  
<sup>b</sup> See Supplementary Data 1 for measurements used to calculate inventories.

338 ± 244 m (1 SD). The average surface elevation at coring locations were higher for regressive sites (0.36 ± 0.25 m NAVD88; 1 SD) than transgressive sites (0.16 ± 0.07 m NAVD88; 1 SD;  $p = 0.01$ ) excluding outlier regressive site SRE-D (Table 1). The carbon content of the salt marsh units generally decreased with depth and from the surface to ~20 cm depth was higher at transgressive than regressive sites (Fig. 3; Supplementary Data 1). Salt marsh CAR was measured on a subset of the cores (22) by measuring the carbon stock ( $C_s$ ; g C m<sup>-2</sup>), constraining the period during which the carbon stock accumulated ( $C_p$ ; years) by radiocarbon dating the base of the salt marsh peat and inspecting historical aerial photographs (see methods), and applying the equation  $CAR = C_s/C_p$ . Sites with multiple dates along the transect show that the age of transgressive and regressive marsh units increase and decrease towards the basin, respectively.

**Temporal and Spatial Changes in Salt Marsh CAR.** Salt marsh CAR is directly linked with the rate of RSLR, which accelerated from 0.9 mm yr<sup>-1</sup> to 2.4 mm yr<sup>-1</sup> at the end of the 19th century at our sample locations<sup>8,23,38,39</sup> (Fig. 4). The first salt marsh to colonize the substrate ranges in age from 772 to 15-years, extending across the period of accelerating sea-level rise. We binned CAR values into measurements made over periods >120-years from present ( $n = 13$ ) that includes salt marsh strata that formed during slow and rapid sea-level rise and <120 years from present that includes salt marsh strata that formed entirely during rapid sea-level rise ( $n = 9$ ), with present being the year of core collection (Table 1). For the transgressive and regressive salt marshes that initially formed >120 years ago, mean CAR was 41.1 ± 17.2 g C m<sup>-2</sup> yr<sup>-1</sup> (1 SD) and increased with decreasing formation age following an exponential relationship (Fig. 4). The change in CAR through time is mainly the result of the younger salt marsh units being composed of proportionately less degraded organic material that accumulated more rapidly than the older salt marsh units. As RSLR accelerated during the late 19th century, the salt marshes experienced increased flooding, which

stimulated plant growth and promoted carbon-rich sediment accumulation<sup>8,40</sup>. The younger upper strata within the salt marshes that are >120 years in age is composed of carbon-rich sediment that accumulated more rapidly during the 20th century under conditions of rapid RSLR than the older lower salt marsh strata.

The CARs of the nine transgressive and regressive salt marshes that formed since 1900 CE and accumulated carbonaceous sediment only during the period of more rapid RSLR were generally higher and more variable (range = 323.4–13.9 g C m<sup>-2</sup> yr<sup>-1</sup>; mean = 139.4 ± 80.7 g C m<sup>-2</sup> yr<sup>-1</sup>; 1 SD) than the older salt marshes (Fig. 4). The two samples with lower CAR values (<90 g C m<sup>-2</sup> yr<sup>-1</sup>) were obtained from regressive salt marsh NPR-D at the center of the platform and near the upland edge away from the migrating shoreline, and follow that same exponential relationship observed for the older salt marsh units (Fig. 4). The six samples with variable CAR values >112 g C m<sup>-2</sup> yr<sup>-1</sup>, however, are from the youngest transgressive site (NB;  $n = 3$ ), young areas of transgressive salt marshes positioned close to the migrating upland edge (sites JB and LB;  $n = 2$ ), and the youngest area of regressive salt marsh NPR-D close to the migrating salt marsh shoreline ( $n = 1$ ). This suggests spatial variability in CAR, integrated over the last 120 years, exists across salt marsh platforms, and is a product of marsh ontogeny. The young sample from regressive site SRE-D is an exception because it has the lowest CAR of all the salt marsh samples that formed since 1900 CE (55 g C m<sup>-2</sup> yr<sup>-1</sup>), despite it being obtained close to the migrating shoreline (~3 m away) like the core from Site NPR-D with the highest CAR. Unlike the other salt marshes, Site SRE-D is degrading, as evidenced by its low elevation ~40 cm below the other regressive salt marshes (Table 1; Supplementary Fig. 1).

The CAR values are high in the young transgressive salt marsh (Site NB), near the landward edge of transgressive salt marshes that have been in existence for centuries (sites JB and LB), and near the seaward edge of young regressive salt marshes (Site NPR-D but not degrading salt marsh SRE-D; Fig. 4). Neither



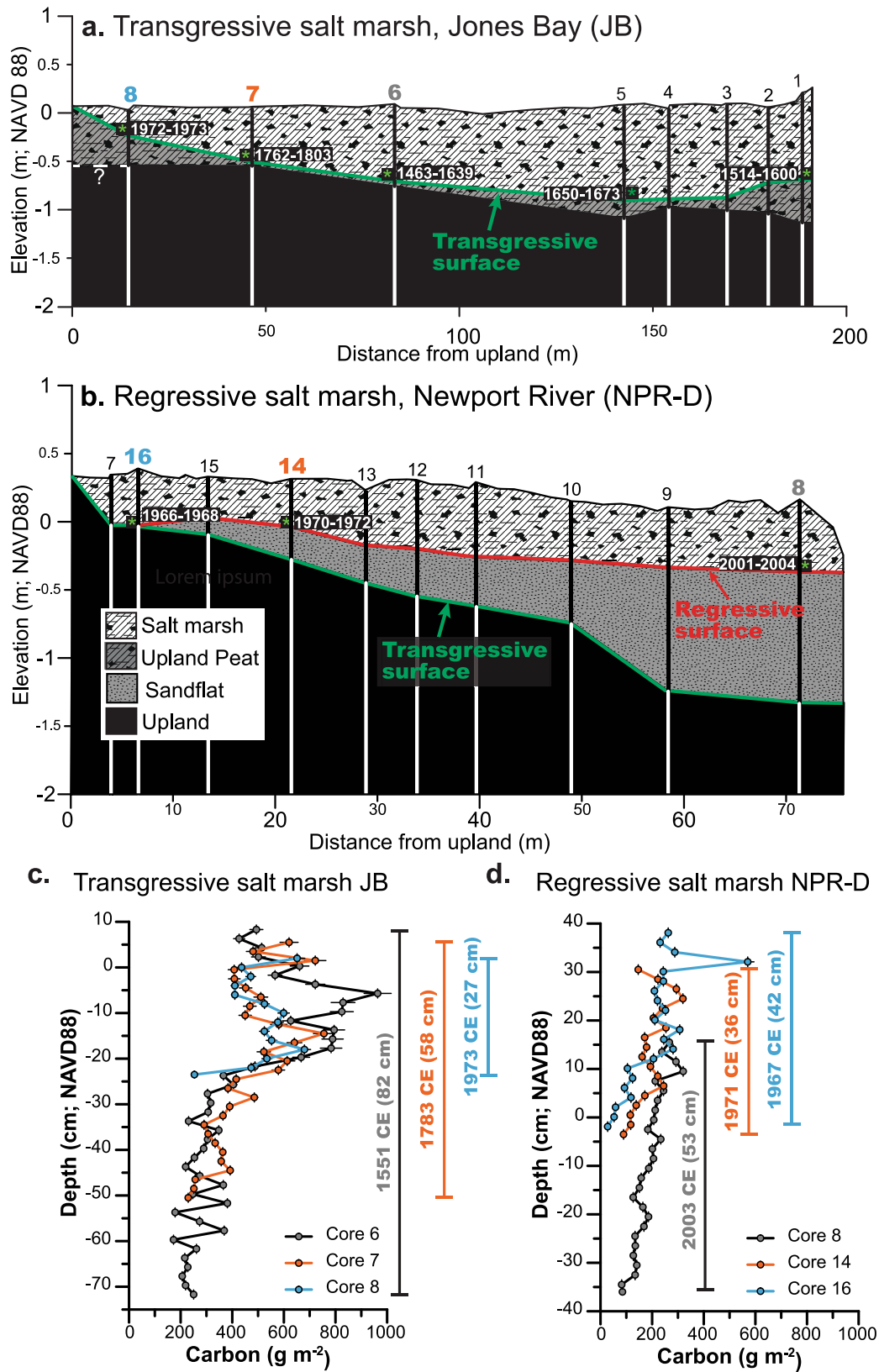


**Fig. 3** Marsh stratigraphy and carbon profiles. Transgressive and regressive salt marshes show a deepening-upward<sup>35</sup> (a) and shallowing-upward (b) sequence of depositional environments, respectively. The green asterisks mark dates of salt marsh initial colonization. Vertical profiles of carbon at transgressive site Jones Bay (c) and regressive site Newport-downstream (d). See cross sections, above, for profile locations. Points are plotted with bars displaying 95% confidence intervals for carbon and the sampling interval for depth (error bars <symbol size not displayed). See Fig. 2 for transect locations and Supplementary Data 1 for additional information on dates and subsamples.

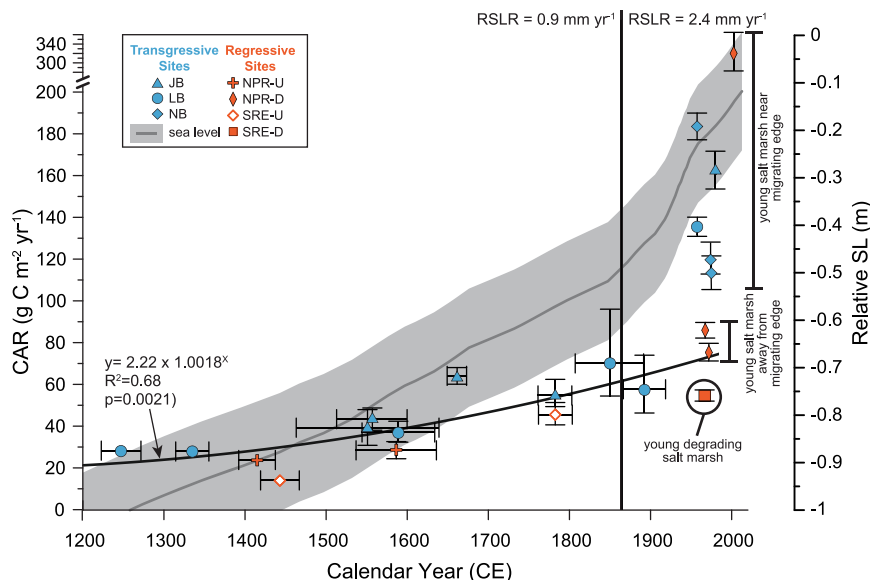


**Fig. 4 Carbon accumulation rates (CAR) of transgressive and regressive salt marshes increase with decreasing age of initial colonization.** At the end of the 19th century, relative sea-level rise (RSLR) accelerated to  $\sim 2.4 \text{ mm yr}^{-1}$  (grey line  $\pm 95\%$  confidence interval)<sup>38</sup> and promoted higher rates of salt marsh vertical accretion and CAR over the last 120 years than previous centuries. The CAR of young salt marsh (<120 years) measured near migrating edges is high and variable due to the greater accommodation from subsidence and water depth at landward and basinward margins, respectively, that promoted rapid accumulation of carbon-rich sediment<sup>35</sup>. Each point on the graph represents an individual core. The exponential curve is based on the samples younger than 1900 CE. Symbols are plotted at the median calibrated age and error bars represent 95% confidence intervals (error bars <symbol size not displayed). Study sites are differentiated by symbols with JB Jones Bay, LB Long Bay, NB Nelson Bay, NPR-U Newport River upstream, NPR-D Newport River downstream, SRE-U Shallotte River Estuary upstream, and SRE-D Shallotte River Estuary downstream. See Fig. 2, Table 1, and Supplementary Data 1 for additional information.

variations in vegetation type nor elevation can explain those observations because at each site vegetation type was consistent among sampling locations, there is no relationship between our measurements of CAR and surface elevation ( $R^2 = 0.02$ ;  $p = 0.53$ ), and the assumption that the marsh surface elevation in relation to the tidal frame was constant from initial colonization to present is not valid for regressive salt marshes. Sediment accommodation is different near migrating edge locations than the middle of the salt marsh platform, where CAR values follow an exponential relationship and sediment accommodation is mainly created by regional RSLR. For transgressive marshes, migration occurs into palustrine wetlands dominated by evergreens (pocosins)<sup>41</sup>. As sea-level inundated the pocosin, soil salinization caused the living root network to die, decay, and subsequently compact, which resulted in localized subsidence<sup>34,42</sup>. That localized subsidence decreased through time<sup>35</sup> and provided sediment accommodation in addition to what was being formed by more regional RSLR. The high CAR values at the young transgressive Site NB and the landward edge of sites LB and JB, which have only been salt marsh since  $\sim 1957$  CE, resulted from the salt marsh rapidly infilling accommodation space with carbon-rich sediment over multiple decades.

The other mechanism for marsh area expansion is featured by the regressive salt marsh NPR-D. In this case, migration occurs into the estuary and salt marsh plants initially colonized low unvegetated tidal-flat substrate at the salt marsh plant minimum threshold elevation (Fig. 3). The colonial salt marsh vegetation became established low in the tidal frame where inundation time was high, allogenic sediment supply was high, and accommodation space was high. Those conditions initially led to the rapid accumulation of salt marsh sediment at site NPR-D and elsewhere in the estuary<sup>37</sup> over several decades, thus corresponding to high CAR values integrated over a multi-decadal time scale.

At the leading migrating edge of transgressive and regressive salt marshes, CARs are at a maximum because accommodation space is high and rapid colonization of new substrates preserved carbon by quickly burying organic material and limiting degradation<sup>43</sup>. Eventually, CAR decreases within a static unit of colonial marsh as it matures into interior marsh when its surface accretes to higher elevations within the tidal frame, and the marsh edge continues to transgress or regress away. This is indicated by the lower CAR values measured in the interior marsh, which has been dissociated from the leading edges.

**Temporal and spatial changes in carbon density.** The nature of our approach for studying salt marsh carbon stocks, with a focus on measuring CAR, could be masking other spatial and temporal variations in carbon burial. This is because rapidly accumulating salt marsh with a low carbon content can have the same CAR as a slowly accumulating salt marsh with a high carbon content. To address this, we compared the carbon densities ( $\text{kg C m}^{-3}$ ) of the salt marsh units (see methods). The range of carbon densities varied between  $9.2\text{--}30.1 \text{ kg m}^{-3}$  and the average carbon density of regressive marsh units dominated by *Spartina alterniflora* ( $12.1 \pm 3.2 \text{ kg m}^{-3}$ ; 1 SD) was lower ( $p = 1.4 \times 10^{-6}$ ) than transgressive marsh units dominated by *Juncus rosmarinus* ( $23.6 \pm 3.5 \text{ kg m}^{-3}$ ; 1 SD; Fig. 5). Salt marsh regression requires deposition of lithogenic sediment at the shoreline to raise the elevation of adjacent flats, form intertidal substrate, and make conditions habitable for salt marsh grasses. Salt marsh transgression only requires RSLR; therefore, the greater supply of lithogenic sediment to regressive salt marshes results in overall lower carbon densities as compared to transgressive salt marshes.

Both regressive and transgressive salt marshes had predictable trends in carbon density with age (Fig. 5). The carbon density of regressive marshes was directly related to the age of the unit while

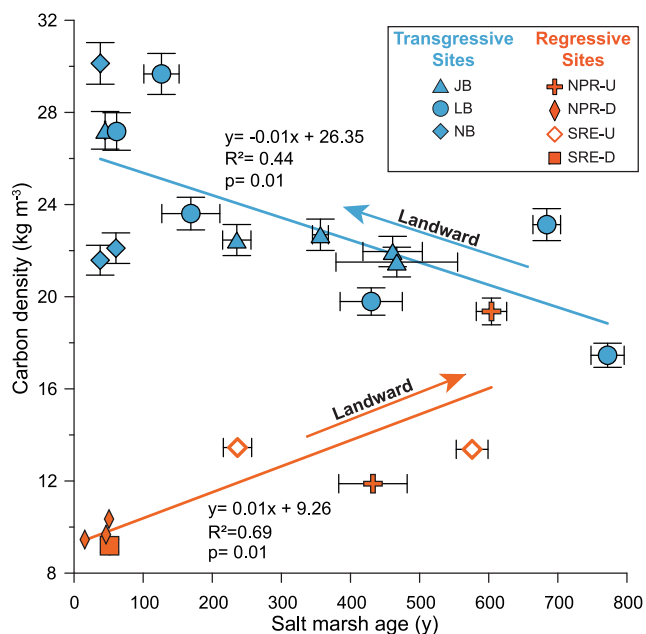


**Fig. 5 Carbon density vs. salt marsh age.** The carbon density of salt marsh sediment is higher in transgressive than regressive salt marshes. As the age of regressive and transgressive salt marshes increased and decreased, respectively, carbon density increased. The oldest areas of regressive salt marshes and the youngest areas of transgressive salt marshes are positioned at the upland boundary, indicating the carbon density of salt marsh sediment progressively increases in a landward direction from the estuary. Shapes are plotted at median values and error bars represent 95% confidence intervals (error bars <symbol size not displayed).

transgressive marshes were inversely related. This shows that carbon densities are highest near the landward edge of both types of fringing salt marsh because the age of regressive and transgressive salt marsh units increase in landward and seaward directions, respectively. The trend of increasing carbon densities in a landward direction is likely due to the different sources of sediment available for salt marsh accretion across the platform. Lithogenic sediment is mainly supplied to all salt marshes from adjacent riverine or estuarine water bodies and is preferentially deposited near the shoreline causing sediment concentrations of floodwater to decrease landward<sup>44</sup>. In contrast to shoreline areas, the landward edge of fringing salt marsh near the upland is supplied with more organic carbon from a variety of sources in addition to decaying grass, such as leaf litter from the forest canopy<sup>45</sup> and wrack deposited during storms<sup>46</sup>.

Carbon budgets for coastal areas and salt marsh carbon stock assessments commonly disregard temporal and spatial variations in CAR across and among salt marshes<sup>17,18</sup>. The spatial and temporal trends in salt marsh CAR, documented here, should exist globally when superimposed on the large-scale variability from differing latitude and tidal range<sup>17</sup>. Along the shoreline of regressive salt marshes where salt marsh grasses colonize low-elevation substrate and the landward edge of transgressive salt marshes where soil salinization causes increased subsidence, CARs are >200% higher than interior locations where the salt marsh units are older. Additionally, CARs are higher in younger marsh units because of accelerating RSLR at the end of the 19th century that promoted rapid accumulation of carbon-rich sediment. Salt marsh areas influenced by accelerating RSLR, high subsidence rates at the landward edge, and that recently established on low-elevation substrate near the shoreline have abundant vertical space within the intertidal niche that is rapidly

filled with carbon-rich sediment. Those conditions are conducive to high CARs but only to a point. There is an upper limit to the rate of RSLR that a vertically accreting salt marsh can keep up with<sup>13</sup>, and when exceeded the salt marsh will experience increased erosion, lose much of its carbon stock, and transition to a subtidal flat seascape.

The landward edge of transgressive salt marshes and seaward edge of regressive salt marshes have the highest CARs, and these areas are severely impacted by humans. Armoring the landward edge of salt marsh with a bulkhead or revetment prevents transgression, removes the upland transition zone where we documented some of the highest CARs, and increases erosion<sup>47,48</sup>. In 2010, 14% of the tidal shoreline in the U.S.A. was hardened and that number is expected to double by 2100 CE<sup>49</sup>. Salt marsh shoreline erosion is increasing due to human impacts that are shifting estuarine conditions towards higher hydrodynamic energy from increased boat wakes<sup>50</sup> and dredging activities<sup>51</sup>. In addition, wave attenuation in estuaries has been reduced from the loss of shallow-water foundation species such as submerged aquatic vegetation<sup>52</sup> and oyster reefs<sup>53</sup>, which makes salt marshes less resistant to erosion during storm events<sup>54</sup>. Anthropogenic modification of watersheds can increase sedimentation in estuaries<sup>55</sup> and form regressive marshes that would not exist in a natural state, and if sediment loads decrease in the future, these young salt marshes will likely deteriorate<sup>56</sup>. Scaling salt marsh restoration and conservation efforts to offset a specific amount of greenhouse gas emissions should not be based on average CAR values for a given region because salt marsh ontogeny, age, landscape setting, and proximity to the upland drive the large spatial and temporal range of CARs and carbon densities. Projections of salt marsh carbon stocks and burial rates with accelerating sea-level rise<sup>57</sup> and growing coastal populations must include information on the spatial and temporal variability of CARs to be accurate.

## Methods

**Site location and sampling.** North Carolina has ~800 km<sup>2</sup> of salt marsh mainly fringing estuarine shorelines<sup>38</sup>. North of Cape Lookout (CL), the slope of the upland forest along estuarine shorelines is generally lower (~0.004) than south of CL (~1.0). As sea level rose during the Holocene and inundated upland areas, the difference in lower coastal plain morphology promoted wide (>200 m) and narrow (<80 m) fringing salt marshes to form northeast and west of CL, respectively. We chose three transgressive salt marsh sites north of CL with ramp-like upland boundaries where the salt marsh progressively colonized coastal forest, including Jones Bay (JB), Long Bay (LB), and Nelson Bay (NB)<sup>35</sup> (Fig. 2 and Supplementary Fig. 1). We also chose two regressive sites south of CL with scarp-like upland boundaries where salt marsh expanded into the estuary and progressively colonized mud flats, including Newport River (NPR) and Shallotte River (SR). At the regressive sites, we sampled along two transects positioned in the upstream (U) and downstream (D) parts of the estuary. The sites north of CL and NPR-U were composed mostly of *J. roemerianus* with a thin (<5 m) rim of *S. alterniflora* at the seaward boundary and the samples came from areas composed of *J. roemerianus*. NPR-D and SR-D were composed of only *S. alterniflora* and SR-U is mostly *S. alterniflora* with a narrow (<5 m) rim of *J. roemerianus* at the upland boundary and the samples came from areas composed of *S. alterniflora*.

Each transect of cores extended perpendicular from the salt marsh shoreline to the upland boundary. The salt marsh surface elevation along the transects and the position of each core was surveyed using a Trimble R8 RTK-GPS receiver and the North Carolina Virtual Reference System with an average vertical error ±2–3 cm and horizontal error of <1 cm. Cores were collected using a 7.6 cm diameter aluminum irrigation pipe connected to a cement vibrator and averaged 3 m in length. All 55 cores we collected for the study sampled the entire salt marsh unit.

**Sample processing.** Cores were split in half lengthwise, one half was used for measuring the amount of organic matter in the sediment, and the other half was photographed, described, and subsampled for foraminifera and plant material for radiocarbon dating. All subsamples were collected from the center of the core to avoid contamination with material that may have been displaced along the interior surface of the tube during the coring process. Cores with upland peat below the salt marsh peat were subsampled at 1 cm (1 cm<sup>3</sup>) intervals for the presences of foraminifera to identify the contact between the two units<sup>35</sup>. Subsamples were washed with deionized water through a 2 mm sieve to separate larger plant matter and

through a 63 µm sieve to separate foraminifera. Samples were then inspected wet under a microscope.

We subsampled 8 cm<sup>3</sup> at the base of the salt marsh peat unit for radiocarbon dating from 14 transgressive marsh cores (six at JB, eight at LB, and four at NB) and eight regressive marsh cores (three at NPR-D, two at NPR-U, two at SR-U, and one at SR-D). We chose stems or leaves that were horizontal in the core for analysis to ensure subsamples were preserved in-situ. The National Ocean Sciences Accelerator Mass Spectrometry Facility at Woods Hole Oceanographic Institution radiocarbon dated the subsamples, and we calibrated the ages to calendar years using CALIB 7.1<sup>59,60</sup> or CALIBomb<sup>61,62</sup>. Many of the calibrated dates provided multiple possible date ranges (2 SD) and we generally chose date ranges with the highest certainty unless other information, like stratigraphic position or aerial photography provided a better estimate. Salt marsh age is the difference between the year of core collection (2018 or 2019; see Table 1) and the date of initial colonization.

To determine the organic content of the salt marsh sediment, we used the loss on ignition (LOI) method<sup>63</sup>. The cores were subsampled continuously by slicing 8 cm<sup>3</sup> cubes out of the center of the cores. In some instances, at the base of the salt marsh, subsamples were <8 cm<sup>3</sup> to avoid including underlying material in the measurement. Subsamples were dried at ~105 °C for at least 16 h before being weighed to obtain an initial dry mass (g). Samples were then combusted at 550 °C for 4 h and then weighed again to obtain ignited mass. The LOI (%) was calculated using the equation: ((dry mass-ignited mass)/dry mass) × 100. The percent organic matter from LOI was converted to percent organic carbon (C<sub>Craft</sub>) using the regression equation: (0.40 ± 0.01) LOI + (0.0025 ± 0.0003) LOI<sup>2</sup><sup>64</sup> developed from salt marsh samples obtained close to our sites. The percent organic carbon of each subsample was converted to g C m<sup>-2</sup> by: (((C<sub>Craft</sub>/100) × dry mass)/sample volume) × 10,000. To calculate the carbon stock sampled in each salt marsh core, we summed the carbon measurements of the continuous subsamples (g C m<sup>-2</sup>) to the base of the salt marsh unit. Carbon density (kg m<sup>-3</sup>) is the carbon stock divided by the thickness of the salt marsh unit and the carbon accumulation rate is the carbon stock divided by the age of the salt marsh.

**Reporting summary.** Further information on research design is available in the Nature Research Reporting Summary linked to this article.

## Data availability

The data set that supports the findings of this study, including radiocarbon and down-core profiles of loss on ignition and dry bulk density is available in Supplementary Data 1 and in the Figshare online open access repository at <https://doi.org/10.6084/m9.figshare.20137649.v265>.

Received: 20 January 2022; Accepted: 15 July 2022;

Published online: 02 August 2022

## References

- Kollmuss, A., Zink, H. & Polycarp, C. *Making Sense of the Voluntary Carbon Market: a Comparison of Carbon Offset Standards* (WWF Germany, 2008).
- Kelley, J. J. et al. A national approach to greenhouse gas abatement through blue carbon management. *Global Environmental Change* **63**, 102083 (2020).
- Wang, F. et al. Global blue carbon accumulation in tidal wetlands increases with climate change. *Natl. Sci. Rev.* <https://doi.org/10.1093/nsr/nwaa296> (2021).
- Macreadie, P. I. et al. The future of blue carbon science. *Nat. Commun.* **10**, 3998 (2019).
- McLeod, E. et al. A blueprint for blue carbon: toward an improved understanding of the role of vegetated coastal habitats in sequestering CO<sub>2</sub>. *Front. Ecol. Environ.* **9**, 552–560 (2011).
- Chmura, G. L., Anisfeld, S. C., Cahoon, D. R. & Lynch, J. C. Global carbon sequestration in tidal, saline wetland soils. *Global Biogeochem. Cycles* **17**, 1111 (2003).
- Holmquist, J. R. et al. Accuracy and precision of tidal wetland soil carbon mapping in the conterminous United States. *Sci. Rep.* **8**, 9478, <https://doi.org/10.1038/s41598-018-26948-7> (2018).
- McTigue, N. et al. Sea level rise explains changing carbon accumulation rates in a salt marsh over the past two millennia. *JGR Biogeosci.* **124**, 2945–2957 (2019).
- McTigue, N. D., Walker, Q. A. & Currin, C. A. Refining estimates of greenhouse gas emissions from salt marsh “blue carbon” erosion and decomposition. *Front. Marine Sci.* <https://doi.org/10.3389/fmars.2021.661442> (2021).
- Pendleton, L. et al. Estimating global “blue carbon” emissions from conversion and degradation of vegetated coastal ecosystems. *PLoS One* **7**, e43542 (2012).
- Theuerkauf, E. J., Stephens, J. D., Ridge, J. T., Fodrie, F. J. & Rodriguez, A. B. Carbon export from fringing saltmarsh shoreline erosion overwhelms carbon storage across a critical width threshold. *Estuarine, Coast. Shelf Sci.* **164**, 367–378 (2015).
- Lovelock, C. E. et al. Assessing the risk of carbon dioxide emissions from blue carbon ecosystems. *Front. Ecol. Environ.* **15**, 257–265 (2017).
- Morris, J. T., Sundareshwar, P. V., Niench, C. T., Kjerfve, B. & Cahoon, D. R. Responses of coastal wetlands to rising sea level. *Ecology* **83**, 2869–2877 (2002).
- Kirwan, M. L., Temmerman, S., Skeehean, E. E., Guntenspergen, G. R. & Fagherazzi, S. Overestimation of marsh vulnerability to sea level rise. *Nat. Clim. Change* **6**, 253–260 (2016).
- Teal, J. M. & Kanwisher, J. *Gas Exchange in a Georgia Saltmarsh*. <https://doi.org/10.4319/lo.1961.6.4.0388> (1961).
- Howarth, R. W. & Teal, J. M. Sulfate reduction in a New England salt marsh. *Limnol. Oceanogr.* **24**, 999–1013 (1979).
- Ouyang, X. & Lee, S. Y. Updated estimates of carbon accumulation rates in coastal marsh sediments. *Biogeosciences* **11**, 5057–5071, <https://doi.org/10.5194/bg-11-5057-2014> (2014).
- Wilkinson, G. M., Besterman, A., Buelo, C., Gephart, J. & Pace, M. L. A synthesis of modern organic carbon accumulation rates in coastal and aquatic inland ecosystems. *Sci. Rep.* **8**, 15736 (2018).
- Rovira, P. & Vallejo, V. R. Labile and recalcitrant pools of carbon and nitrogen in organic matter decomposing at different depths in soil: an acid hydrolysis approach. *Geoderma* **107**, 109–141 (2002).
- Darby, F. A. & Turner, R. E. Below- and aboveground *Spartina alterniflora* production in a Louisiana salt marsh. *Estuaries Coast.* **31**, 223–231 (2008).
- Breithaupt, J. L. et al. Avoiding timescale bias in assessments of coastal wetland vertical change. *Limnol. Oceanogr.* **63**, S477–S495 (2018).
- Rogers, K. et al. Wetland carbon storage controlled by millennial-scale variation in relative sea-level rise. *Nature* **567**, 91–95 (2019).
- Breithaupt, J. L. et al. Increasing rates of carbon burial in southwest Florida coastal wetlands. *JGR Biogeosci.* <https://doi.org/10.1029/2019jg005349> (2020).
- Gehrels, W. R. & Woodworth, P. L. When did modern rates of sea-level rise start. *Glob. Planetary Change* **100**, 263–277 (2013).
- Rodriguez, A. B. & McKee, B. A. in *Salt Marshes: Function, Dynamics, and Stresses* (Cambridge University Press, 2021).
- Broome, S. W., Seneca, E. D. & Woodhouse, W. W. Tidal salt marsh restoration. *Aquatic Botany* **32**, 1–22 (1988).
- Williams, P. & Faber, P. Salt marsh restoration experience in San Francisco Bay. *J. Coast. Res.* **27**, 203–211 (2001).
- Wolters, M., Garbutt, A. & Bakker, J. P. Salt marsh restoration: evaluating the success of de-embankments in north-west Europe. *Biol. Conservation* **123**, 249–268 (2005).
- Mitchell, M. & Bilkovic, D. M. Embracing dynamic design for climate-resilient living shorelines. *J. Appl. Ecol.* **56**, 1099–1105 (2019).
- Davis, C. A. Salt marsh formation near Boston and its geological significance. *Econ. Geol.* **5**, 623–639 (1910).
- Redfield, A. C. Ontogeny of a salt marsh estuary. *Science* **147**, 50–55 (1965).
- Fagherazzi, S. et al. Sea level rise and the dynamics of the marsh-upland boundary. *Front. Environ. Sci.* <https://doi.org/10.3389/fenvs.2019.00025> (2019).
- Schieder, N. W. & Kirwan, M. L. Sea-level driven acceleration in coastal forest retreat. *Geology* **47**, 1151–1155 (2019).
- Charles, S. P. et al. Experimental saltwater intrusion drives rapid soil elevation and carbon loss in freshwater and brackish everglades marshes. *Estuaries Coast.* **42**, 1868–1881 (2019).
- Miller, C. B., Rodriguez, A. B. & Bost, M. C. Sea-level rise, localized subsidence, and increased storminess promote salt marsh transgression across low-gradient upland areas. *Quaternary Sci. Rev.* **265**, 107000 (2021).
- Fagherazzi, S., Carniello, L., D’Alpaos, L. & Defina, A. Critical bifurcation of shallow microtidal landforms in tidal flats and salt marshes. *Proc. Natl. Acad. Sci.* **103**, 8337–8341 (2006).
- Gunnell, J. R., Rodriguez, A. B. & McKee, B. A. How a marsh is built from the bottom up. *Geology* **41**, 859–862 (2013).
- Kemp, A. C. et al. The relative utility of foraminifera and diatoms for reconstructing late Holocene sea-level change in North Carolina, USA. *Quat. Res.* **71**, 9–21 (2017).
- Herbert, E. R., Windham-Myers, L. & Kirwan, M. L. Sea-level rise enhances carbon accumulation in United States tidal wetlands. *One Earth* <https://doi.org/10.1016/j.oneear.2021.02.011> (2021).
- Kirwan, M. L. & Murray, A. B. Ecological and morphological response of brackish tidal marshland to the next century of sea level rise: Westham Island, British Columbia. *Glob. Planetary Change* **60**, 471–486 (2007).
- Brinson, M. M. Landscape properties of pocosins and associated wetlands. *Wetlands* **11**, 441–465, <https://doi.org/10.1007/bf03160761> (1991).



42. DeLaune, R. D., Nyman, J. A. & Patrick Jr, W. Peat collapse, ponding and wetland loss in a rapidly submerging coastal marsh. *J. Coast. Res.* **10**, 1021–1030 (1994).
43. Choi, Y. & Wang, Y. Dynamics of carbon sequestration in a coastal wetland using radiocarbon measurements. *Global Biogeochem. Cy.* <https://doi.org/10.1029/2004gb002261> (2004).
44. Stumpf, R. P. The process of sedimentation on the surface of a salt marsh. *Estuarine, Coast. Shelf Sci.* **17**, 495–508 (1983).
45. McKee, K. L. & Faulkner, P. L. Restoration of biogeochemical function in mangrove forests. *Restoration Ecol.* **8**, 247–259 (2000).
46. Cahoon, D. R. A review of major storm impacts on coastal wetland elevations. *Estuaries Coast.* **29**, 889–898 (2006).
47. Doody, J. P. ‘Coastal squeeze’—an historical perspective. *J. Coast. Conserv.* **10**, 129 (2004).
48. Gehman, A.-L. M. et al. Effects of small-scale armoring and residential development on the salt marsh-upland ecotone. *Estuaries Coast.* **41**, 54–67 (2018).
49. Gittman, R. K. et al. Engineering away our natural defenses: an analysis of shoreline hardening in the US. *Front. Ecol. Environ.* **13**, 301–307 (2015).
50. Manis, J. E., Garvis, S. K., Jachec, S. M. & Walters, L. J. Wave attenuation experiments over living shorelines over time: a wave tank study to assess recreational boating pressures. *J. Coast. Conserv.* **19**, 1–11 (2015).
51. Cox, R., Wadsworth, R. A. & Thomson, A. G. Long-term changes in salt marsh extent affected by channel deepening in a modified estuary. *Cont. Shelf Res.* **23**, 1833–1846 (2003).
52. Donatelli, C., Ganju, N. K., Kalra, T. S., Fagherazzi, S. & Leonardi, N. Changes in hydrodynamics and wave energy as a result of seagrass decline along the shoreline of a microtidal back-barrier estuary. *Adv. Water Res.* **128**, 183–192 (2019).
53. Zu Ermgassen, P. S. E. et al. Historical ecology with real numbers: past and present extent and biomass of an imperilled estuarine habitat. *Proc. Royal Soc. B: Biol. Sci.* **279**, 3393–3400 (2012).
54. Angelini, C., Altieri, A. H., Silliman, B. R. & Bertness, M. D. Interactions among foundation species and their consequences for community organization, biodiversity, and conservation. *Bioscience* **61**, 782–789 (2011).
55. Rodriguez, A. B., McKee, B. A., Miller, C. B., Bost, M. C. & Atencio, A. N. Coastal sedimentation across North America doubled in the 20th century despite river dams. *Nat. Commun.* <https://doi.org/10.1038/s41467-020-16994-z> (2020).
56. Mattheus, C. R., Rodriguez, A. B. & McKee, B. A. Direct connectivity between upstream and downstream promotes rapid response of lower coastal-plain rivers to land-use change. *Geophys. Res. Lett.* <https://doi.org/10.1029/2009GL039995> (2009).
57. Rahmstorf, S. A semi-empirical approach to projecting future sea-level rise. *Science* **315**, 368–370 (2007).
58. Sutter, L. *DCM Wetland Mapping in Coastal North Carolina*. 45 (Division of Coastal Management, North Carolina Department of Environment and Natural Resources, 1999).
59. Stuiver, M. & Reimer, P. J. Extended 14C database and revised CALIB radiocarbon calibration program. *Radiocarbon* **35**, 215–230 (1993).
60. Reimer, P. J. et al. IntCal13 and Marine13 Radiocarbon age calibration curves 0–50,000 years cal BP. *Radiocarbon* **55**, 1869–1887, [https://doi.org/10.2458/azu\\_js\\_rc.55.16947](https://doi.org/10.2458/azu_js_rc.55.16947) (2013).
61. Reimer, P. J., Brown, T. A. & Reimer, R. W. Discussion: reporting and calibration of post-bomb 14C data. *Radiocarbon* **46**, 1299–1304 (2004).
62. Reimer, R.W. & Reimer, P.J. 2020 CALIBomb [WWW program]. <http://calib.org> (2020).
63. Heiri, O., Lotter, A. F. & Lemcke, G. Loss on ignition as a method for estimating organic and carbonate content in sediments: reproducibility and comparability of results. *J. Paleolimnol.* **25**, 101–110 (2001).
64. Craft, C., Seneca, E. & Broome, S. Loss on ignition and Kjeldahl digestion for estimating organic carbon and total nitrogen in estuarine marsh soils: calibration with dry combustion. *Estuaries* **14**, 175–179 (1991).
65. Rodriguez, A., Miller, C., & Bost, M. Salt marsh radiocarbon and loss on Ignition data. figshare. *Dataset.* <https://doi.org/10.6084/m9.figshare.20137649.v2> (2022).

## Acknowledgements

Research was supported by the North Carolina Sea Grant (R/18-HCE-3) and the Department of Defense Environmental Security Technology Certification Program (RC19 D3 5218).

## Author contributions

A.B.R. and C.B.M. participated in all aspects of the study. M.C.B. helped collect, process, and interpret data and edit the manuscript. B.A.M. and N.D.M. provided feedback on the analysis and interpretation and edited the manuscript.

## Competing interests

The authors declare no competing interests.

## Additional information

**Supplementary information** The online version contains supplementary material available at <https://doi.org/10.1038/s43247-022-00501-x>.

**Correspondence** and requests for materials should be addressed to Antonio B. Rodriguez.

**Peer review information** *Communications Earth & Environment* thanks Faming Wang and the other, anonymous, reviewer(s) for their contribution to the peer review of this work. Primary handling editors: Lei Chen and Clare Davis. Peer reviewer reports are available.

**Reprints and permission information** is available at <http://www.nature.com/reprints>

**Publisher's note** Springer Nature remains neutral with regard to jurisdictional claims in published maps and institutional affiliations.



**Open Access** This article is licensed under a Creative Commons Attribution 4.0 International License, which permits use, sharing, adaptation, distribution and reproduction in any medium or format, as long as you give appropriate credit to the original author(s) and the source, provide a link to the Creative Commons license, and indicate if changes were made. The images or other third party material in this article are included in the article's Creative Commons license, unless indicated otherwise in a credit line to the material. If material is not included in the article's Creative Commons license and your intended use is not permitted by statutory regulation or exceeds the permitted use, you will need to obtain permission directly from the copyright holder. To view a copy of this license, visit <http://creativecommons.org/licenses/by/4.0/>.

© The Author(s) 2022